

STRUCTURE AND MAGNETIC PROPERTIES OF Ni-Al AND Ni-Mn-Al COMPOUND PRODUCED BY ARC MELTING

Bambang SOEGIJONO¹, Hamdan Akbar NOTONEGORO², Jan SETIAWAN³

In this paper, we trace the structure and magnetic properties of Ni-Al and Ni-Mn-Al compound produced by Arc melting. Tracing have been done by comparing the structure and magnetic properties of Ni₃Al, Ni₂MnAl and Ni₅₀Mn₃₂Al₁₈ alloys system. Analysis structure on Ni₂MnAl show that the atomic position of Mn and Al are at different site. But for Ni₅₀Mn₃₂Al₁₈, the atomic position of Mn and Al occupy the same site. Ni₃Al and Ni₂MnAl do not show ferromagnetic phenomena, but Ni₅₀Mn₃₂Al₁₈ alloys system have shown ferromagnetic phenomena. It could be expected that one of the Ni-Mn-Al system (Ni₅₀Mn₃₂Al₁₈) could a parental compound for magnetocaloric materials by partial substitute of Al by Mn in its lattice.

Keywords: Ni-Mn-Al, parental compound, magnetocaloric, alloy.

1. Introduction

Nowadays, many researches have been conducted on search of finding new magnetocaloric material base on metal or its alloys. The magnetic refrigerant becomes new cooling technology which is more efficiently and environmental friendly [1,2]. The entropy changes due to magnetization cycle will replace compression cycles to absorb or emitting heat. The material with the magnetocaloric effect (MCE) properties will work for that functionality [2–4]. Many efforts have been made to achieve that goal such as increasing the MCE value to absorb and release heat. In 1976, Gd which has large MCE in near room temperature had been considered to be the most suitable refrigerant [5,6]. Nevertheless, Gd is highly expensive and more toxic for health [7–9].

Since Ni–Mn–Al alloys base on Heusler become the potential candidate for cheaper materials which exhibiting good performance MCE around room temperature, it also has a high strength of the grain boundaries and can be tuned as favorable materials [10–13]. There is something interesting about this Ni-Mn-Al system for magnetocaloric material research. In general, researcher uses Ni₂MnAl as a parental compound, to substitute partially the parts of the alloy [14–18]. But

¹ Universitas Indonesia, Indonesia, E-mail: naufal@ui.ac.id

² Universitas Indonesia, Universitas Sultan Ageng Tirtayasa, Indonesia, E-mail: hamdan_an@untirta.ac.id

³ Badan Tenaga Nuklir Nasional, Indonesia

in last decade, recently found a new trend to uses $\text{Ni}_{50}\text{Mn}_{32}\text{Al}_{18}$ as a parental compound but the question still open. They substitute the part of this alloy to produce the magnetic material MCE which is quite good as a magnetic refrigerant.

Kim *et. al.* reported in their study in the $\text{Ni}_{41}\text{Co}_9\text{Mn}_{32}\text{Al}_{18}$ quaternary alloy system shows the optimal value at 10 kOe to provide $|\Delta S_M|^{pk}$ of $2.1 \text{ J kg}^{-1} \text{ K}^{-1}$ observed at 300 K. These values generate the refrigerant capacity (RC) as 52 J kg^{-1} of that material [19]. Furthermore, Kim *et. al.* also investigated the $\text{Ni}_{1.7}\text{Co}_{0.3}\text{Mn}_{1.26}\text{Al}_{0.74}$ alloy system that similar with $\text{Ni}_{42.5}\text{Co}_{7.5}\text{Mn}_{31.5}\text{Al}_{18.5}$. In this material, they could generate the value of $|\Delta S_M|^{pk}$ as $2.1 \text{ J kg}^{-1} \text{ K}^{-1}$ which gave refrigerant capacity value (RC) of 49 J kg^{-1} at $\Delta H = 10 \text{ kOe}$ [20]. In other way, Xuan *et. al.* found that in the $\text{Ni}_{44}\text{Fe}_6\text{Mn}_{32}\text{Al}_{18}$ alloy system obtained the value of magnetic entropy change as $3.35 \text{ J kg}^{-1} \text{ K}^{-1}$ at $\Delta H = 30 \text{ kOe}$ [21]. In the opposite, Xuan *et. al.* also found that in the $\text{Ni}_{42}\text{Co}_8\text{Mn}_{32}\text{Al}_{18}$ alloy system generate the value of $|\Delta S_M|^{pk}$ as $7.7 \text{ J kg}^{-1} \text{ K}^{-1}$ and got under $\Delta H = 60 \text{ kOe}$ that capacity of the effective refrigerant value of 112 J kg^{-1} , more than Kim *et. al.* founded [22].

Therefore, in this research, we trace the magnetic properties and structure of off-stoichiometric $\text{Ni}_{50}\text{Mn}_{32}\text{Al}_{18}$ alloy system, from the features of Ni_3Al , which is binary alloys system, and the properties of Ni_2MnAl which is full Heusler alloy system. By this mean, the beneficial of $\text{Ni}_{50}\text{Mn}_{32}\text{Al}_{18}$ as the parental compound become more seen.

2. Methods

The series of Ni-Mn-Al alloy samples were prepared in proportional composition (at. %) from pure powder metals (99% pro analysis) using arc melting furnace with argon atmosphere. In a sealed quartz glass tube, the ingots were annealed at 900°C for 48 hours and cooling gradually at room temperature.

Powder X-ray diffractometer using $\text{Cu-K}\alpha$ radiation was conducted to identify the crystal structure and to characterize the phases present at room temperature. Rietveld analysis by GSAS and Visualization for Electronic and Structural Analysis (VESTA) software also used to model the atomic structure. The field dependence of magnetization (J - H) was measured at 25°C with an applied magnetic field (H_{ext}) 600 kA/m using PERMAGRAPH®-L MAGNET-PHYSIK Dr. Steingroever GmbH.

3. Result and discussion

The X-Ray Diffraction pattern of Ni_3Al , Ni_2MnAl , and $\text{Ni}_{50}\text{Mn}_{32}\text{Al}_{18}$ alloys system are shown in Fig 1, 2 and 3. Ni_3Al alloys consist of two-phase as shown in Fig. 1, which are cubic structure and space group (Pm-3m) also known as the *fcc* and tetragonal (P4/mmm) structures [23].

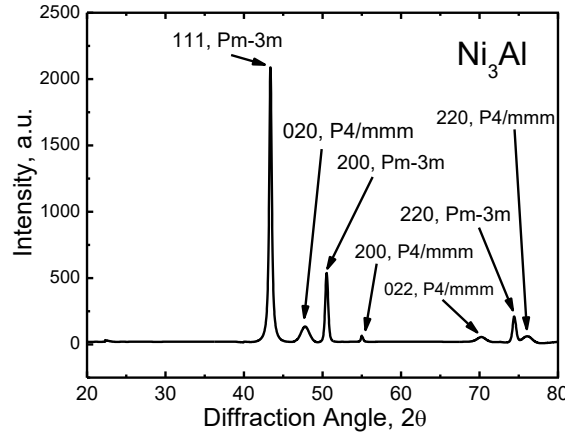


Fig.1 XRD pattern of Ni_3Al Alloy system. There is two phase structure present, Cubic *fcc* (s.g. Pm-3m) and tetragonal (s.g. P4/mmm).

Then, Fig. 2 shows that Ni_2MnAl alloys compound consist of two-phase, which are cubic (Fm-3m) as $\text{L}2_1$ type structure and cubic *fcc* (Pm-3m) structures belonging to Ni_3Al present [24–26,23]. We can identified the $\text{L}2_1$ structure as Heusler Alloy system from the reflection of (111), (200), and (220) [27].

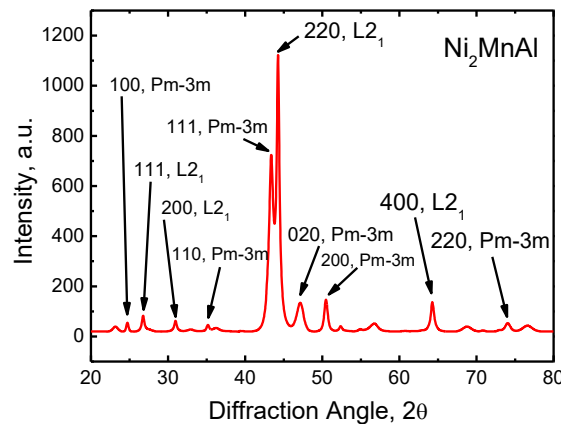


Fig.2 XRD pattern of Ni_2MnAl Alloy system which consist of two-phase structure, $\text{L}2_1$ (fm-3m) and Ni_3Al (Pm-3m).

Moreover, in Fig.3 appear the phase structure of $\text{Ni}_{50}\text{Mn}_{32}\text{Al}_{18}$ alloy system consist of single cubic *fcc* structure (Pm-3m). This structure were identified from the reflection of (100), (111), (200), and (220) as obvious intensity, and the reflection of (110), (210), and (211) which are tiny.

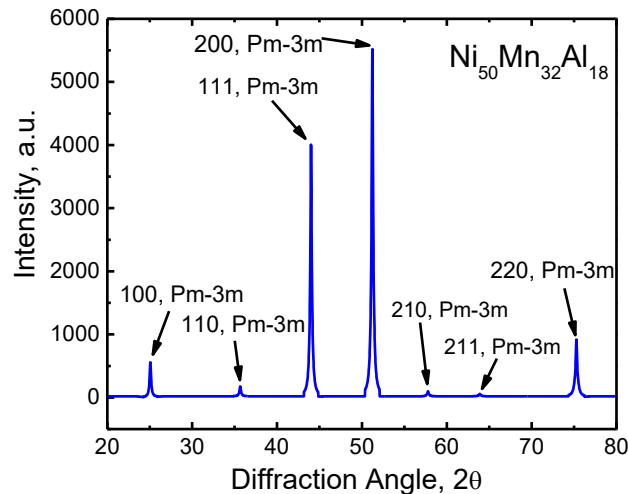


Fig.3 XRD pattern of $\text{Ni}_{50}\text{Mn}_{32}\text{Al}_{18}$ Alloy system which consist of single-phase Cubic *fcc* and space group (Pm-3m)

We can see in Table 1 that the structure of L2_1 formation has volume much larger than the cubic *fcc* (Pm-3m) and tetragonal (P4/mmm) phase structures but has mass density much smaller than two other phase structures.

Tabel 1
Phase structure of alloys system Ni_3Al , Ni_2MnAl , dan $\text{Ni}_{50}\text{Mn}_{32}\text{Al}_{18}$

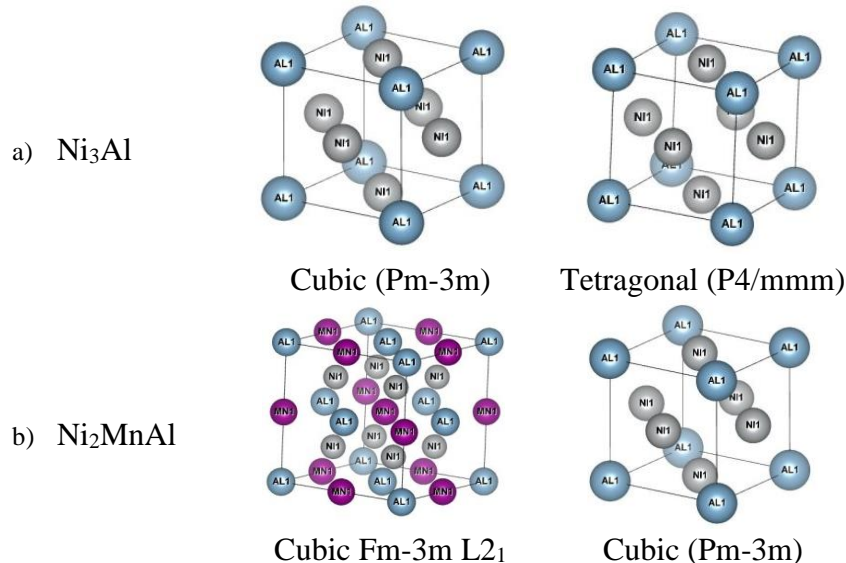
Compound	Phase structure	S.G.	$a=b=c$ (Å)	$\alpha=\beta=\gamma$	V (Å ³)	Density (gr/cm ³)
Ni_3Al	Tetragonal	P4/mmm	3.795 3.795 3.325	90°	47.909	7.04
	Cubic	Pm-3m	3.602	90°	46.744	7.21
Ni_2MnAl	Cubic L2_1 (Ni_2MnAl)	Fm-3m	5.811	90°	196.296	6.74
	Cubic (Ni_3Al)	Pm-3m	3.629	90°	47.795	7.05
$\text{Ni}_{50}\text{Mn}_{32}\text{Al}_{18}$	Cubic	Pm-3m	3.575	90°	45.700	7.68

Table 2 shows the present position of Ni_2 atoms of Ni_3Al alloys in tetragonal phase structure (P4/mmm), which also found in Ni_2MnAl with cubic phase structure (Fm-3m). The Mn atom and Al atom occupies different position. Meanwhile, the present position of Mn1 atoms and Al atom in $\text{Ni}_{50}\text{Mn}_{32}\text{Al}_{18}$ alloy system occupy the same position with site occupancy 0.64 and 0.36 respectively.

Tabel 2
Atomic Position of alloy system $\text{Ni}_{75}\text{Al}_{25}$, $\text{Ni}_{50}\text{Mn}_{25}\text{Al}_{25}$, and $\text{Ni}_{50}\text{Mn}_{32}\text{Al}_{18}$

Compound	S.G.	Posisi atom (x,y,z)			
		Ni1	Ni2	Mn1	Al1
Ni_3Al	P4/mmm	2e (0, 0.5, 0.5)	1c (0.5, 0.5, 0)	-	1a (0, 0, 0)
	Pm-3m	3c (0, 0.5, 0.5)	-	-	1a (0, 0, 0)
Ni_2MnAl	Fm-3m	8c (0.25, 0.25, 0.25)	4b (0.25, 0.25, 0.25)	4b (0.5, 0.5, 0.5)	4a (0, 0, 0)
	Pm-3m (Ni_3Al)	3c (0, 0.5, 0.5)	-	-	1a (0, 0, 0)
$\text{Ni}_{50}\text{Mn}_{32}\text{Al}_{18}$	Pm-3m	3c (0, 0.5, 0.5)	-	1a (0, 0, 0) SOF 0.64	1a (0, 0, 0) SOF 0.36

In Fig.4 shown the structure of the 3-dimensional simulation which based on data from Rietveld analysis results of Ni_3Al , Ni_2MnAl , $\text{Ni}_{50}\text{Mn}_{32}\text{Al}_{18}$ alloys system. In Ni_3Al alloys, both phases structures, cubic *fcc* (Pm-3m) and tetragonal (P4/mmm), seem almost identical (Fig.4a). both phases are distinguished by the ratio of the lattice length of the tetragonal phase structure (P4/mmm). In Fig.4b we can see the present formation of $\text{L}2_1$ cubic (Fm-3m) structure. In Fig.4c also shows that the formation of a single phase in $\text{Ni}_{50}\text{Mn}_{32}\text{Al}_{18}$ alloys which has *afcc* cubic (Pm-3m) phase structure.



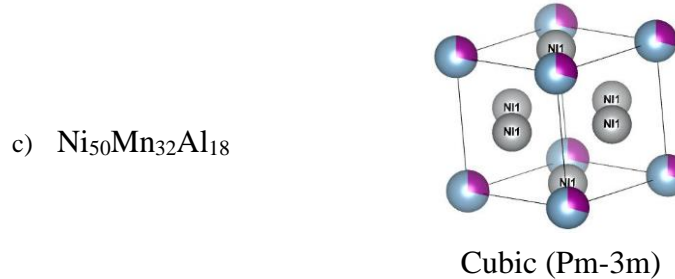


Fig. 4 The *Vesta* simulation of the unit cell of the crystalline structure of a) Ni_3Al , b) Ni_2MnAl , and c) $\text{Ni}_{50}\text{Mn}_{32}\text{Al}_{18}$ alloy system.

Fig. 5 shows the results of magnetization of binary alloy Ni_3Al alloys, to tertiary of Ni_2MnAl alloys, and $\text{Ni}_{50}\text{Mn}_{32}\text{Al}_{18}$ by the external field. The Ni_3Al magnetization curve had conduct a negative linear slope which shows the diamagnetic properties (Fig.5a). The magnetization of Ni_2MnAl curve also shows the forms of negative linear slope (Fig.5b). However, the presence of the $\text{L}2_1$ phase structure in alloys compound has decreased the diamagnetic properties in Ni_2MnAl alloys. Then, a magnetization curve of $\text{Ni}_{50}\text{Mn}_{32}\text{Al}_{18}$ alloys in Fig.5c shows the ferromagnetic properties of the compound. It appears that the magnetization curve conduct a positive value and reaches saturation of $J = 0.06$ T at $H = 600$ kA/m with a small remanence ($6.21 \cdot 10^{-4}$ T) and coercivity ($2.5 \cdot 10^{-5}$ kA/m).

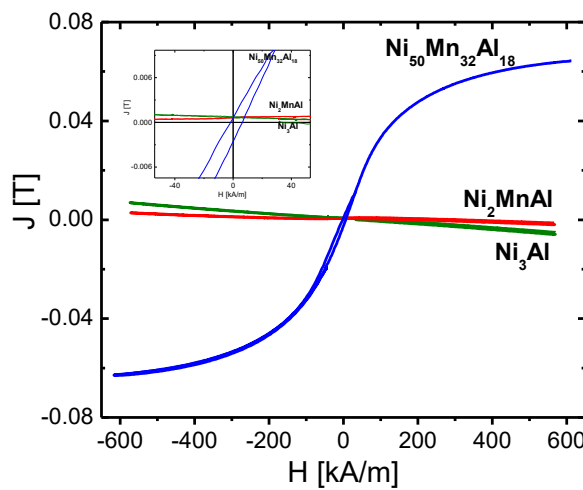


Fig. 5 Magnetic hysteresis curve of a) $\text{Ni}_{75}\text{Al}_{25}$, b) $\text{Ni}_{50}\text{Mn}_{25}\text{Al}_{25}$, and c) measured at 25 °C. Inset shows the small remanence ($6.21 \cdot 10^{-4}$ T) and coercivity ($2.5 \cdot 10^{-5}$ kA/m) of $\text{Ni}_{50}\text{Mn}_{32}\text{Al}_{18}$ alloys system.

From the results above that the revealed magnetic properties of each alloy is divided into two major magnetic domains, that is:

- Diamagnetic, which are consists of Ni_3Al and $\text{Ni}_2\text{MnAl}/\text{Ni}_{50}\text{Mn}_{25}\text{Al}_{25}$.
- Ferromagnetic, belongs to $\text{Ni}_{50}\text{Mn}_{32}\text{Al}_{18}$ alloys which have cubic *fcc* single phase structure (Pm-3m).

From these results, it is shown that $\text{Ni}_{50}\text{Mn}_{32}\text{Al}_{18}$ alloy could be used as a parental compound among the possible Ni-Mn-Al alloy systems. The magnetic properties of the $\text{Ni}_{50}\text{Mn}_{32}\text{Al}_{18}$ could be enhanced by partial substitute of Mn with other ferromagnetic element such as Cobalt. It is expected that substitution of these parental compound will be obtained the cubic phase structure of *fcc* or cubic L_2 [20,28]. Then, the alloy have ferromagnetic properties at room temperature. It may be possible to search another compound from Ni-Mn-Al system to be another parental compound.

6. Conclusions

From the above results, that the ferromagnetic $\text{Ni}_{50}\text{Mn}_{32}\text{Al}_{18}$ had shown with single phase structure of *fcc* cubic (Pm-3m). The use of $\text{Ni}_{50}\text{Mn}_{32}\text{Al}_{18}$ alloys as the parent composition becomes very reasonable. Partial substitution to this compound would obtain to adjust magnetic parameters to conduct the ferromagnetic properties of the alloy system. $\text{Ni}_{50}\text{Mn}_{32}\text{Al}_{18}$ become a new trend as a parental compound to produce magnetic material MCE which quite good as a magnetic refrigerant.

Acknowledgements

This work was supported by the Ministry of Research, Technology and Higher Education Republic of Indonesia (contract No. 1011.6/D3/PG/2016) and also partially supported by Universitas Sultan Ageng Tirtayasa – Republic of Indonesia.

R E F E R E N C E S

- [1] Yu B, Gao Q, Zhang B, Meng XZ, Chen Z. Review on research of room temperature magnetic refrigeration. *Int J Refrig* 2003;26:622–36. doi:10.1016/S0140-7007(03)00048-3.
- [2] Zhong W, Au C-T, Du Y-W. Review of magnetocaloric effect in perovskite-type oxides. *Chinese Phys B* 2013;22:057501. doi:10.1088/1674-1056/22/5/057501.
- [3] Pecharsky VK, Gschneidner Jr KA. Magnetocaloric effect and magnetic refrigeration. *J Magn Magn Mater* 1999;200:44–56. doi:10.1016/S0304-8853(99)00397-2.
- [4] Tishin AM, Spichkin YI. Recent progress in magnetocaloric effect: Mechanisms and potential applications. *Int J Refrig* 2014;37:223–9. doi:10.1016/j.ijrefrig.2013.09.012.
- [5] V. Brown G. Magnetic heat pumping near room temperature. *J Appl Phys* 1976;47:3673. doi:<http://dx.doi.org/10.1063/1.323176>.
- [6] Liu H, Liu Z, Li G, Ma X. Magnetic and magnetocaloric properties of ferromagnetic shape memory alloy $\text{Mn}_{50}\text{Ni}_{40}\text{In}_{10-x}\text{Sbx}$. *Solid State Commun* 2016;243:23–7. doi:10.1016/j.ssc.2016.06.005.
- [7] Ghodhbanea S, Dhahri A, Dhahri N, Hlil EK, Dhahri J. Structural, magnetic and magnetocaloric properties of $\text{La}_{0.8}\text{Ba}_{0.2}\text{Mn}_{1-x}\text{Fe}_{x}\text{O}_3$ compounds with $0.6 \times 6 \times 0.1$. *J Alloys Compd* n.d.;550:358–64. doi:10.1016/j.jallcom.2012.10.087.
- [8] Selmi A, M'nassri R, Cheikhrouhou-Koubaa W, Chniba Boudjada N, Cheikhrouhou A. Effects of

partial Mn-substitution on magnetic and magnetocaloric properties in $\text{Pr}_{0.7}\text{Ca}_{0.3}\text{Mn}_{0.95}\text{X}_{0.05}\text{O}_3$ (Cr, Ni, Co and Fe) manganites. *J Alloys Compd* 2015;619:627–33. doi:10.1016/j.jallcom.2014.09.078.

[9] Huang L, Cong DY, Ma L, Nie ZH, Wang MG, Wang ZL, et al. Large magnetic entropy change and magnetoresistance in a $\text{Ni}_{41}\text{Co}_{9}\text{Mn}_{40}\text{Sn}_{10}$ magnetic shape memory alloy. *J Alloys Compd* 2015;647:1081–5. doi:10.1016/j.jallcom.2015.06.175.

[10] Maniraj M, D'Souza SW, Rai A, Schlagel DL, Lograsso TA, Chakrabarti A, et al. Unoccupied electronic structure of Ni_2MnGa ferromagnetic shape memory alloy. *Solid State Commun* 2015;222:1–4. doi:10.1016/j.ssc.2015.08.003.

[11] Roy T, Gruner ME, Entel P, Chakrabarti A. Effect of substitution on elastic stability, electronic structure and magnetic property of Ni–Mn based Heusler alloys: An ab initio comparison. *J Alloys Compd* 2015;632:822–9. doi:10.1016/j.jallcom.2015.01.255.

[12] Santos JD, Sanchez T, Alvarez P, Sanchez ML, Llamazares JLS, Hernando B, et al. Microstructure and magnetic properties of $\text{Ni}_{50}\text{Mn}_{37}\text{Sn}_{13}$ Heusler alloy ribbons. *J Appl Phys* 2008;103:2008–10. doi:10.1063/1.2832330.

[13] Maziarz W, Czaja P, Czeppe T, Góral a., Litynska-Dobrzynska L, Major Ł, et al. Structure And Martensitic Transformation in $\text{Ni}_{44}\text{Mn}_{43.5}\text{Sn}_{12.5-x}\text{Al}_x$ Heusler Alloys. *Arch Metall Mater* 2013;58:6–9. doi:10.2478/amm-2013-0015.

[14] Agarwal S, Stern-Taulats E, Mañosa L, Mukhopadhyay PK. Effect of low temperature annealing on magneto-caloric effect of Ni–Mn–Sn–Al ferromagnetic shape memory alloy. *J Alloys Compd* 2015;641:244–8. doi:10.1016/j.jallcom.2015.04.069.

[15] Paduani C, Migliavacca A, Pöttker WE, Schaf J, Krause JC, Ardisson JD, et al. A study of $\text{Fe}_{2+x}\text{Mn}_{1-x}\text{Al}$ alloys: Structural and magnetic properties. *Phys B Condens Matter* 2007;398:60–4. doi:10.1016/j.physb.2007.04.068.

[16] Rhee JY, Kudryavtsev Y V., Lee YP. Optical property and electronic structures of Ni_2MnAl alloy. *J Magn Magn Mater* 2004;272–276:2003–4. doi:10.1016/j.jmmm.2003.12.497.

[17] Ghosh A, Mandal K. Tuning of magnetocaloric potential in disordered Ni–Mn–Sn alloy. *Phys Procedia* 2014;54:10–5. doi:10.1016/j.phpro.2014.10.030.

[18] Ersoy H, Sandratskii L, Dederichs P, Eriksson O. First-principles study of the exchange interactions and Curie temperature in Heusler alloys. Martin-Luther-Universität Halle-Wittenberg, 2006.

[19] Kim Y, Kim EJ, Choi K, Han WB, Kim HS, Shon Y, et al. Room-temperature magnetocaloric effect of Ni–Co–Mn–Al Heusler alloys. *J Alloys Compd* 2014;616:66–70. doi:10.1016/j.jallcom.2014.07.034.

[20] Xu X, Ito W, Tokunaga M, Kihara T, Oka K, Umetsu R, et al. The Thermal Transformation Arrest Phenomenon in NiCoMnAl Heusler Alloys. *Metals (Basel)* 2013;3:298–311. doi:10.3390/met3030298.

[21] Xuan HC, Zhang YQ, Li H, Han PD, Wang DH, Du YW. The martensitic transformation and magnetic properties in $\text{Ni}_{50-x}\text{Fe}_{x}\text{Mn}_{32}\text{Al}_{18}$ ferromagnetic shape memory alloys. *Appl Phys A* 2015;119:597–602. doi:10.1007/s00339-015-8997-3.

[22] Xuan HC, Chen FH, Han PD, Wang DH, Du YW. Intermetallics Effect of Co addition on the martensitic transformation and magnetocaloric effect of Ni e Mn e Al ferromagnetic shape memory alloys 2014;47:31–5. doi:10.1016/j.intermet.2013.12.007.

[23] Paduani C, Migliavacca A, Sebben ML, Ardisson JD, Yoshida MI, Soriano S, et al. Ferromagnetism and antiferromagnetism in $\text{Ni}_{2+x+y}\text{Mn}_{1-x}\text{Al}_{1-y}$ alloys. *Solid State Commun* 2007;141:145–9. doi:10.1016/j.ssc.2006.10.006.

[24] Kainuma R, Gejima F, Sutou Y, Ohnuma I, Ishida K. Ordering, martensitic and ferromagnetic transformations in Ni–Al–Mn Heusler shape memory alloys. *Mater Trans - JIM* 2000;41:943–9.

[25] Acet M, Duman E, Wassermann EF, Mañosa L, Planes A. Coexisting ferro- and antiferromagnetism in Ni 2MnAl Heusler alloys. *J Appl Phys* 2002;92:3867–71. doi:10.1063/1.1504498.

[26] Hoshino T, Fujima N, Asato M. Ab initio study for magnetism in Ni_2MnAl full-Heusler alloy: A cluster expansion approach for total energy. *J Alloys Compd* 2010;504:S534–7. doi:10.1016/j.jallcom.2010.02.057.

[27] Graf T, Felser C, Parkin SSP. Simple rules for the understanding of Heusler compounds. *Prog Solid State Chem* 2011;39:1–50. doi:10.1016/j.progsolidstchem.2011.02.001.

[28] Kim Y, Kim EJ, Choi K, Han WB, Kim HS, Shon Y, et al. Room-temperature magnetocaloric effect of Ni–Co–Mn–Al Heusler alloys. *J Alloys Compd* 2014;616:66–70. doi:10.1016/j.jallcom.2014.07.034.